CATO-2 Deliverable WP 3.6-D03
Progress report on:
Preparation of site specific geodetic remote sensing techniques for ground movement

Prepared by:	Pooja Mahapatra (TU Delft) Peter A. Fokker (TNO)	25.08.2010 14.09.2010
Reviewed by:	Ramon Hanssen (TU Delft)	26.08.2010
Approved by:	J.Brouwer (CATO-2 Director)	

Distribution List

(this section shows the initial distribution list)

External	copies	Internal	copies

Document Change Record

(this section shows the historical versions, with a short description of the updates)

Version	Nr of pages	Short description of change	Pages

Table of Contents

1 Executive Summary

Case studies have been performed in the areas of Roswinkel and Barendrecht, which contain gas fields. The Roswinkel field had been selected to demonstrate the applicability of ground deformation monitoring to the characterization of the reservoir dynamics; the Barendrecht field is a potential CO_2 storage location. Ground deformation in these areas has been measured using Persistent Scatterer Interferometry (PSI). It is shown that these areas have insufficient persistent scatterer (PS) point density for accurate deformation monitoring if PSI is used as a standalone technology. The need for integration with complementary technology to improve monitoring accuracy is demonstrated. GPS receivers can be installed to improve the monitoring itself, or advanced inversion technology can be applied to extract a maximum of information by combining geodetic monitoring with subsurface modelling.

2 Applicable/Reference documents and Abbreviations

2.1 Applicable Documents

(Applicable Documents, including their version, are documents that are the "legal" basis to the work performed)

	Title	Doc nr	Version date
AD-01	Beschikking (Subsidieverlening CATO-2 programma verplichtingnummer 1-6843	ET/ED/9078040	2009.07.09
AD-02	Consortium Agreement	CATO-2-CA	2009.09.07
AD-03	Program Plan	CATO2-WP0.A-D.03	2009.09.29

2.2 Abbreviations

(this refers to abbreviations used in this document)

ASAR	Advanced Synthetic Aperture Radar (on board Envisat)
CAT	Compact Active Transponder
CO_2	Carbon dioxide
DePSI	Delft PS-InSAR
DInSAR	Differential InSAR
Doris	Delft Object-oriented Radar Interferometric Software
DIDP	Double Interpolation and Double Prediction
ERS	European Remote Sensing satellites
GNSS	Global Navigation Satellite System
GPS	Global Positioning System
InSAR	Interferometric SAR
LoS	Line of Sight
PS	Persistent Scatterer
PSC	PS Candidate
PSI	Persistent Scatterer Interferometry
SAR	Synthetic Aperture Radar
SISTEM	Simultaneous and Integrated Strain Tensor EstiMation

3 Persistent Scatterer Interferometry (PSI)

Traditional InSAR is highly sensitive to vertical ground motion due to its steep look angle, and provides a 1D measurement of change in distance along the line of sight of the radar spacecraft. However, noise due to atmospheric delays or loss of coherence in vegetated or high-relief terrain often hamper InSAR measurements that depend on one or a stack of several interferograms.

Atmospheric effects show a strong spatial correlation within each SAR acquisition, but are uncorrelated in time. Conversely, target motion is usually strongly correlated in time and can exhibit different degrees of spatial correlation depending on the phenomenon at hand (e.g. subsidence due to gas extraction, fault displacements, collapsing infrastructure, localized sliding areas). Atmospheric artefacts can be estimated and removed by combining data from long series of SAR images. Persistent Scatterer Interferometry (PSI) identifies and integrates individual radar-bright and radar- phase-stable points (e.g. outcrops and buildings), called persistent scatterers (PS), in a series of SAR images (typically more than 15). Only scatterers slightly affected by both temporal and geometrical decorrelation are selected. Time-dependent surface motions, atmospheric delays, and elevation-error components of the range-change measurement are subsequently separated out using the phase data from these PS [Burgmann 2006].

The stability of these PS targets allows the removal of the spatially uniform atmospheric phase screen (APS) and the estimate of their relative motion with a precision in the order of 1 mm/y for each PS. The quality of APS removal decreases with distance from the reference point, rapidly increasing at lower frequencies. Therefore, the quality of the relative motion estimation of each PS is reduced to 4 to 5 mm/y at relative distances in the order of 20 km [Zerbini 2007].

Ground deformation in the areas of Roswinkel and Barendrecht in the Netherlands was analysed using the Delft Object-oriented Radar Interferometric Software, Doris [Kampes and Usai, 1999], for interferogram generation, and DePSI (Delft PS-InSAR) processing package for PSI processing. The DePSI processing chain is summarised in Figure 1 [Samiei-Esfahany, 2008].

The two pimary steps of DePSI are preliminary estimation and final estimation/densification. During preliminary estimation, the spatial correlation and temporal decorrelation of the atmospheric signal at a network of pixels exhibiting stable temporal phase behaviour (first order PS candidates, PSC1) is used to filter out the atmospheric phase from interferometric phase. The PSC1 are selected using a normalised amplitude dispersion threshold, and an additional set of second order PS candidates (PSC2) is also selected, using a higher threshold. The final estimation step involves the interpolation of a complete atmospheric phase screen (APS), which is subtracted from the phase of the PSC2. The unknown parameters for each PSC2 are estimated, and the final PS points are selected based on a quality threshold. Therefore, the initial network of PSC1 is effectively densified by the PSC2.

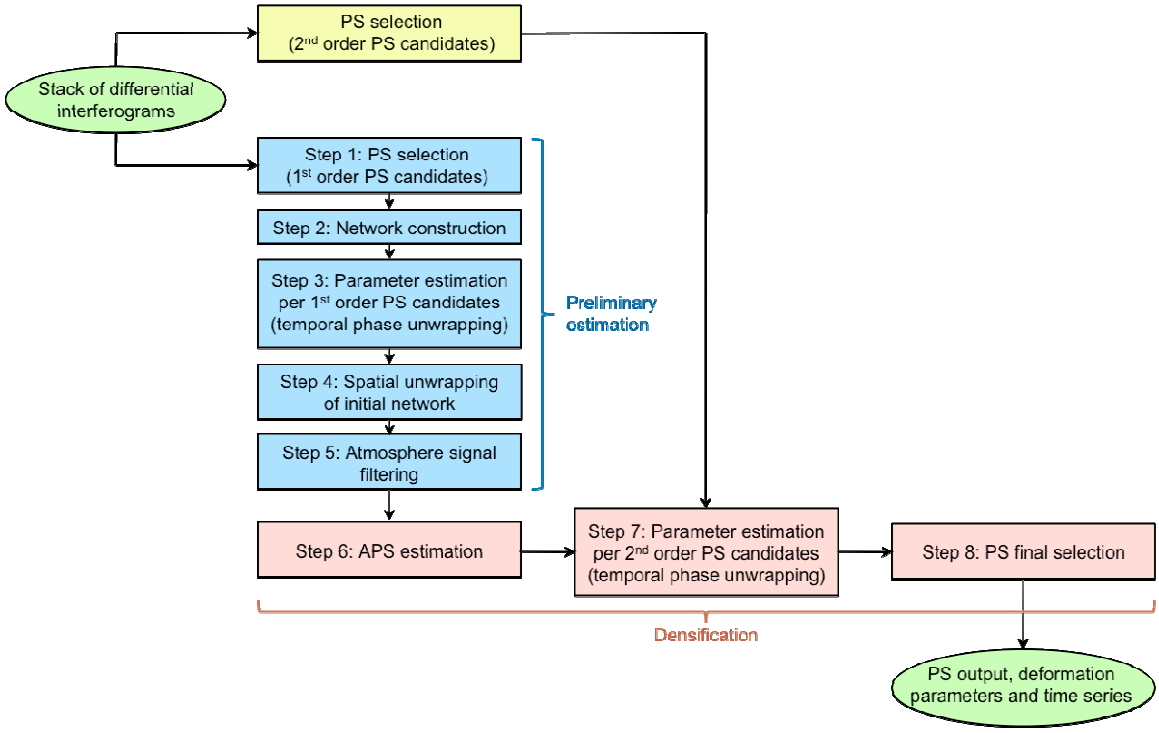

Figure 1. PSI processing chain.

The following considerations are important to note while analysing the results of PSI:

1. Relative nature of deformation estimates: All deformation estimates and rates are relative in space to a reference PS in the image. In the time series, all deformations are relative in time to the master image acquisition time. To derive absolute velocities, information about the vertical velocity of the reference PS and the horizontal direction of the motion is needed, and can be obtained from the analysis of GPS data.
2. Line-of-sight (LoS) estimates: All deformation estimates and rates are in the LoS of the satellite (and not in the vertical direction). In other words, PSI measurements are the projection of real 3D displacement vectors (with components in the North, East and upwards directions) into the LoS direction. Equations 1 and 2 of [Samiei-Esfahany et al, 2009] provide more information on the conversion between 3D deformation and satellite LoS deformation.
3. Precision: Based on stochastic analysis of data in non-deforming areas, deformation estimates in the time series have a standard deviation of ~4 mm.

Deformation rates measured by PSI include the contribution of horizontal motions that project into the radar line-of-sight vector. To isolate the vertical component of the deformation, GPS-derived horizontal velocity field can be used to eliminate its contribution to each PSI deformation measurement. The combined use of continuous GPS and multiple PSI data sets obtained from different acquisition geometries and radar satellites will allow for future improvements in the accuracy of ground deformation measurements.

4 The Roswinkel case

4.1 Background

The Roswinkel field has been selected as a study case to demonstrate the applicability of ground deformation monitoring to the characterization of the reservoir dynamics. Even after a long period of production, uncertainties remained about the geological structure and there were indications that the ground movement measurement could shed light on these issues. Inversion technology applied to surface deformation that facilitates in constraining the subsurface uncertainties of this field would be strong support for the usefulness of ground movement monitoring to CO_2 storage operations.

Figure 2. Location of Roswinkel in the Netherlands.

The Roswinkel field is a gas field in the north-eastern part of the Netherlands (Figure 2) which originally held some 24 billion sm^3 of gas at a depth of about 2.1 km. It has been produced between 1980 and 2005, during which ground subsidence of approximately 17 cm has been measured by nine levelling campaigns. The gas field is a complex anticlinal structure with many faults with uncertain fault transmissibilities. As a result, the field consists of up to 30 reservoir compartments [Fokker et al, 2010]. Reservoir engineering studies have indicated the possibility of

residual gas in compartments which had not been fully depleted. A demonstration of the possibility of using surface movement monitoring to constrain the static and dynamic reservoir behaviour would be a strong case for the use of surface movement monitoring for CO_2 storage. Such a study has been carried out with levelling data. The PSI data have been processed and will be incorporated in the continuation of the project.

4.2 Inversion study using levelling data

TNO has worked on the Roswinkel gas production case, as an inverse analogue of CO_2 injection. An integrated study has been performed to better understand the Roswinkel field behaviour using the subsidence measurements available. A structural model was created with the geological information available - mainly seismics and log data. Various techniques were tried out to estimate the properties of the faults found. The uncertainty present in the geological description has been propagated to a reservoir simulation study. Here, the faults that were expected to have an important contribution to the behaviour of the field were selected and given variable properties. With a Monte Carlo sampling, 100 realizations were created in which these properties constituted the variable parameters. With the rate constraints as measured in the production life of the field, the simulations were performed. Their outcome was judged according to the measured profiles. 87 of the realizations were considered acceptable in view of the predicted rates and pressures. The 87 realizations have been used as prior information in an inversion study using the available levelling measurements above Roswinkel.

The compaction profiles from the 87 realizations showed a variation of about 40% in their values (Fig. 3). Furthermore, the average (expected) profile was relatively smooth and extended well into the lateral aquifer. The available geological and reservoir engineering knowledge did not give a more constrained picture of the reservoir.

The inversion result shows a compaction field that is much better defined (Figure 4): the uncertainty has been reduced to about 10%. The resulting compaction field, and the associated pressure drop, shows a larger depletion in the eastern part of the reservoir due to the apparent sealing of some of the faults. Further, the compaction does not extend far into the aquifer. The conclusion of this study is that surface monitoring can facilitate the identification of reservoir properties and the associated dynamic behaviour. The areas from where the gas had been produced could be localized with considerable accuracy. This implies that the same technology can be applied to localize areas where CO_2 is stored if sufficient surface movement signal can be measured. However, the incorporation of all the available subsurface information is key in this process. In the present study, the fault properties could only be quantified by virtue of the knowledge of their existence and their location.

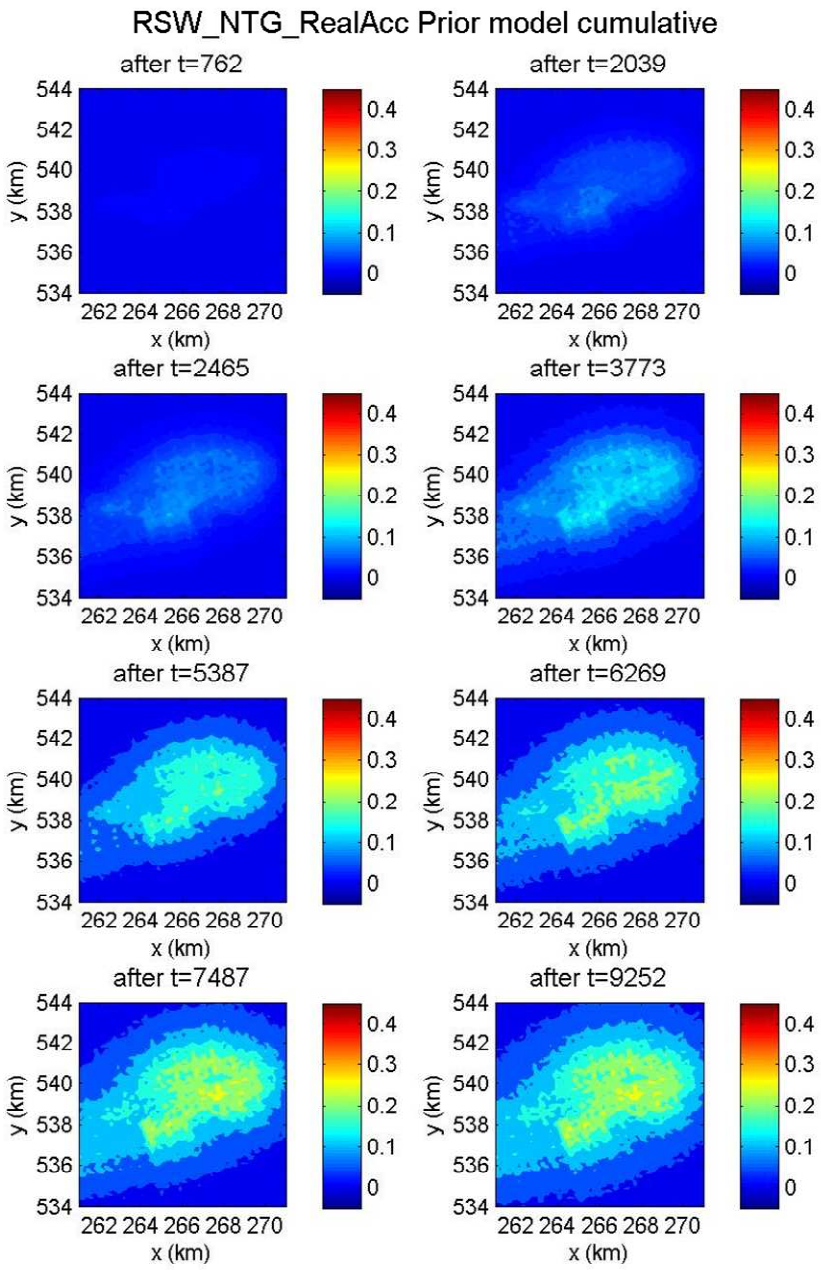

Figure 3. Average compaction field for Roswinkel based on all geological and reservoir knowledge except subsidence (prior field) for different times during production. Note the smooth pattern of the compaction and the absence of observable effect of faults. The scatter around the average is about 40%.

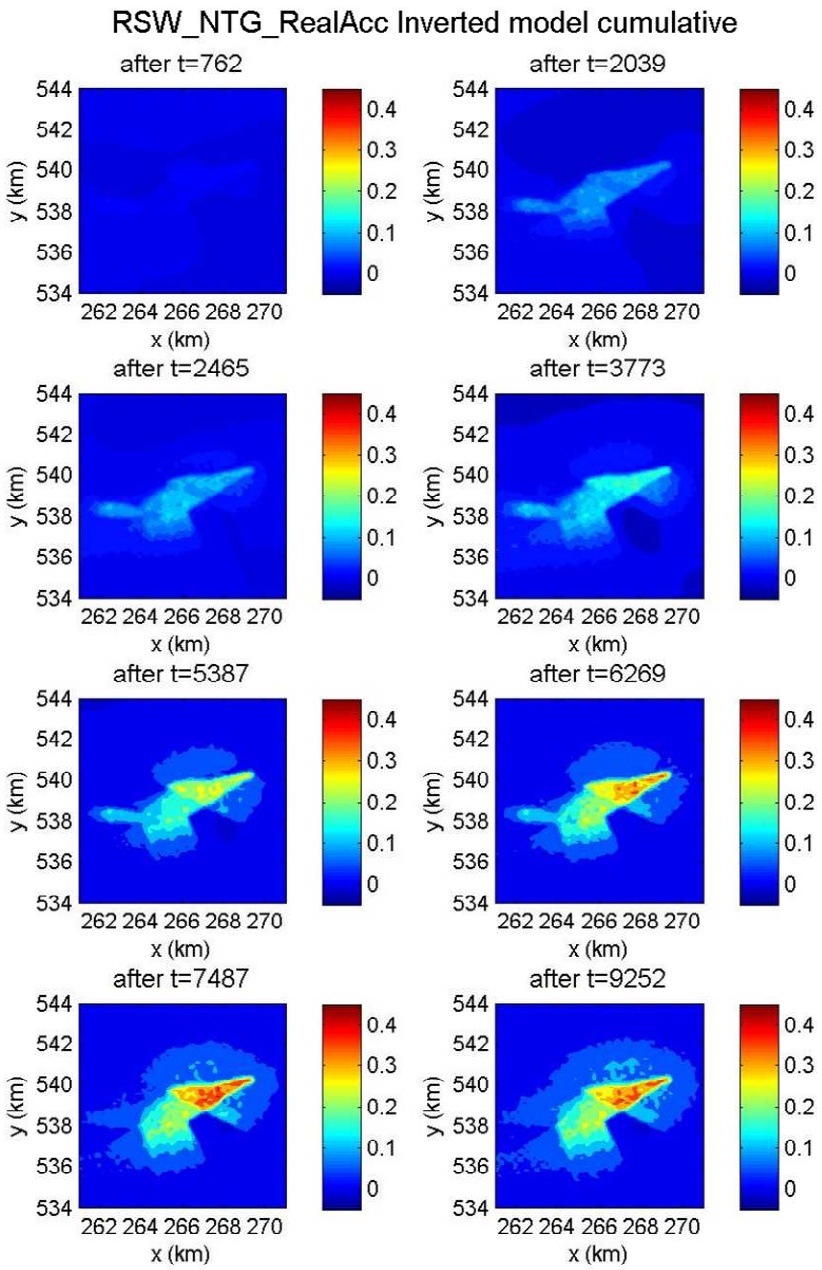

Figure 4. Average compaction field for Roswinkel after the inversion exercise for the same times during production as in Fig. 3. Note the localization of the compaction and the apparent sealing of a number of the faults. The scatter around the average is about 10%.

4.3 PSI processing of Roswinkel (ERS, 1992-2000)

A 20 km x 20 km area centred at the Roswinkel gas reservoir (52.82°N, 7.01°E) was selected for study using Persistent Scatterer Interferometry (PSI). Figure 5 provides an overview of the terrain characteristics of this area. It is observed that large parts of this area are rural.

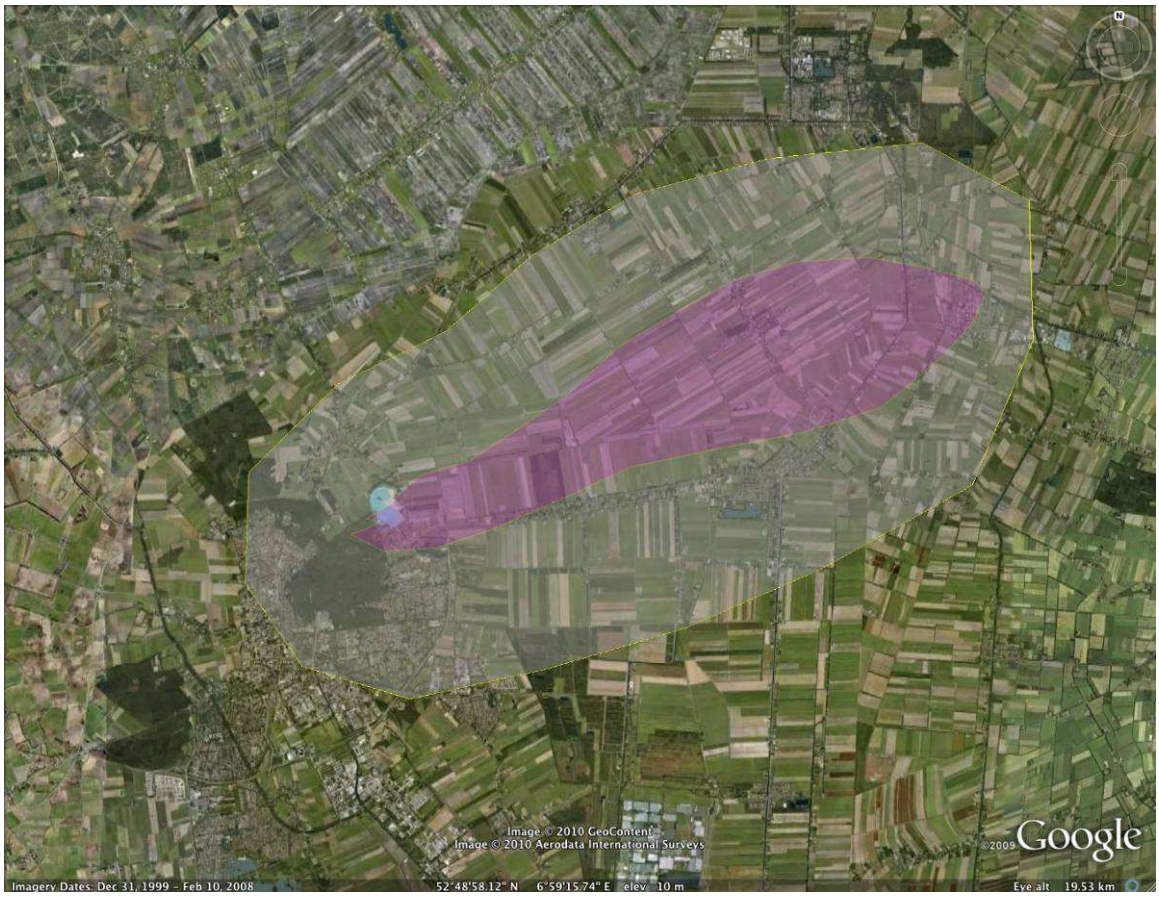

Figure 5. PSI study area: Roswinkel gas field and its surroundings. The area in pink denotes the actual reservoir, and the translucent area around it denotes the zone of expected subsidence.

ERS data in the period 1992-2000 over the area of Groningen were used to study the deformation in the Roswinkel area. As can be seen in Figure 6, only two of the six ERS tracks covering the Groningen area include Roswinkel: the descending track 380 of frame 253, and the ascending track 215 of frame 1063. Each track was processed using interferometric combinations that refer to a common master. The master was selected based on the stack coherence and the geographic ground coverage. Since the amplitude observations of acquisitions with a deviating Doppler centroid frequency deteriorate the PS selection based on normalised amplitude dispersion [Ketelaar, 2008], acquisitions with a Doppler frequency difference larger than 350 Hz from the master's Doppler centroid frequency were excluded.

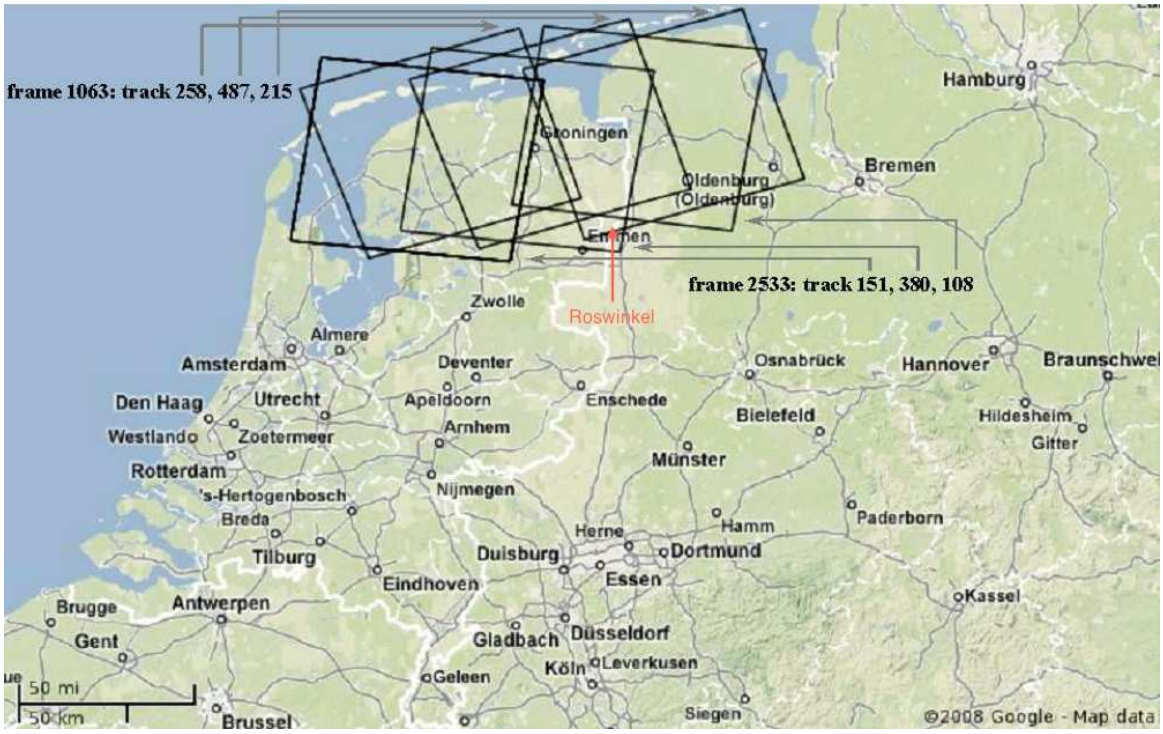

Figure 6. Spatial coverage of the six ERS tracks over the Groningen area of the Netherlands.

76 acquisitions were used for PSI processing of the descending track (master acquisition on 20 Jul 1997, reference point at 53.4702°N and 7.1312°E), and 27 for the ascending track (master acquisition on 14 Jan 1997, reference point at 52.7373°N and 6.8746°E). Table 1 lists the acquisition dates of the SAR images for the descending and ascending tracks.

The respective deformation maps are shown in Figure 7 and Figure 8. The deformation maps using data from the descending and ascending tracks are depicted together, for comparison, in Figure 9. It may be observed in both images that, owing to rural characteristics, the PS density is extremely low in large areas of the subsidence bowl. Also, while comparing the maps in Figure 9, it is important to note that the line-of-sight deformation rates of PS points in the same area measured by the descending and ascending tracks may differ considerably, owing to different look angles of the satellite.

Table 1. Acquisition dates (time series) for ERS descending track 380 (left, master on 20 Jul 1997) and ascending track 215 (right, master on 14 Jan 1997).

	1-May-93
	10-Jul-93
	14-Aug-93
	24-Apr-95

28-May-92	8-Sep-96	8-Apr-96
2-Jul-92	13-Oct-96	9-Apr-96
6-Aug-92	17-Nov-96	17-Jun-96
10-Sep-92	26-Jan-97	18-Jun-96
15-Oct-92	2-Mar-97	22-Jul-96
19-Nov-92	11-May-97	27-Aug-96
24-Dec-92	15-Jun-97	25-Mar-97
28-Jan-93	24-Aug-97	3-Jun-97
4-Mar-93	28-Sep-97	8-Jul-97
8-Apr-93	7-Dec-97	12-Aug-97
13-May-93	11-Jan-98	3-Feb-98
17-Jun-93	15-Feb-98	14-Apr-98
22-Jul-93	22-Mar-98	23-Jun-98
26-Aug-93	26-Apr-98	1-Sep-98
30-Sep-93	31-May-98	19-Jan-99
4-Nov-93	5-Jul-98	30-Mar-99
1-Apr-95	9-Aug-98	7-Jun-99
6-May-95	13-Sep-98	8-Jun-99
10-Jun-95	18-Oct-98	17-Aug-99
15-Jul-95	27-Dec-98	23-May-00
16-Jul-95	31-Jan-99	1-Aug-00
19-Aug-95	7-Mar-99	19-Dec-00
20-Aug-95	11-Apr-99	
23-Sep-95	16-May-99	
29-Oct-95	20-Jun-99	
2-Dec-95	25-Jul-99	
3-Dec-95	29-Aug-99	
6-Jan-96	3-Oct-99	
11-Feb-96	7-Nov-99	
16-Mar-96	12-Dec-99	
17-Mar-96	16-Jan-00	
20-Apr-96	20-Feb-00	
21-Apr-96	26-Mar-00	
25-May-96	30-Apr-00	
26-May-96	22-Oct-00	
3-Aug-96	26-Nov-00	
4-Aug-96	31-Dec-00	

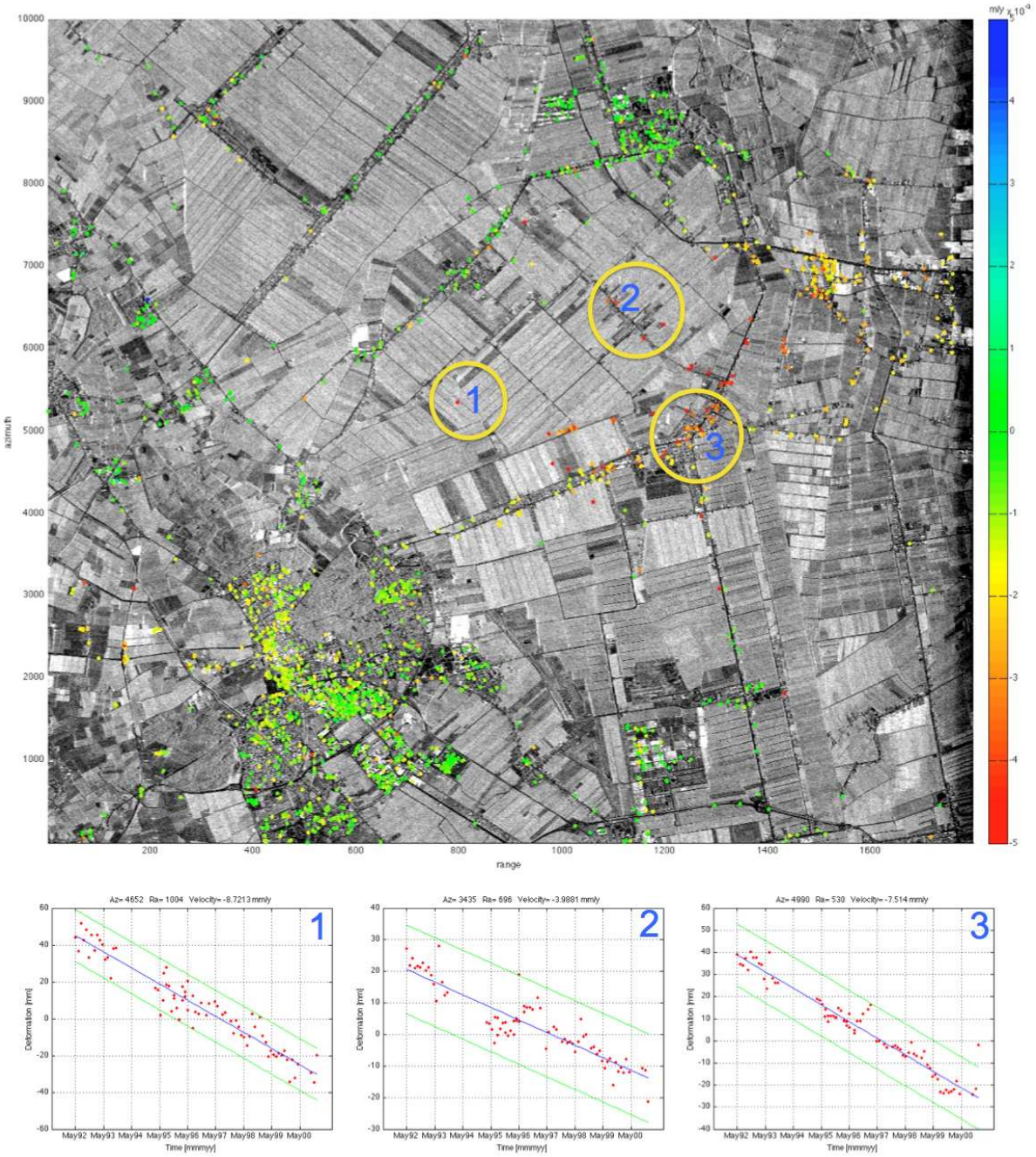

Figure 7. PS deformation map of the Roswinkel area using descending track 215, showing the deformation time series of representative PS points in the subsidence bowl.

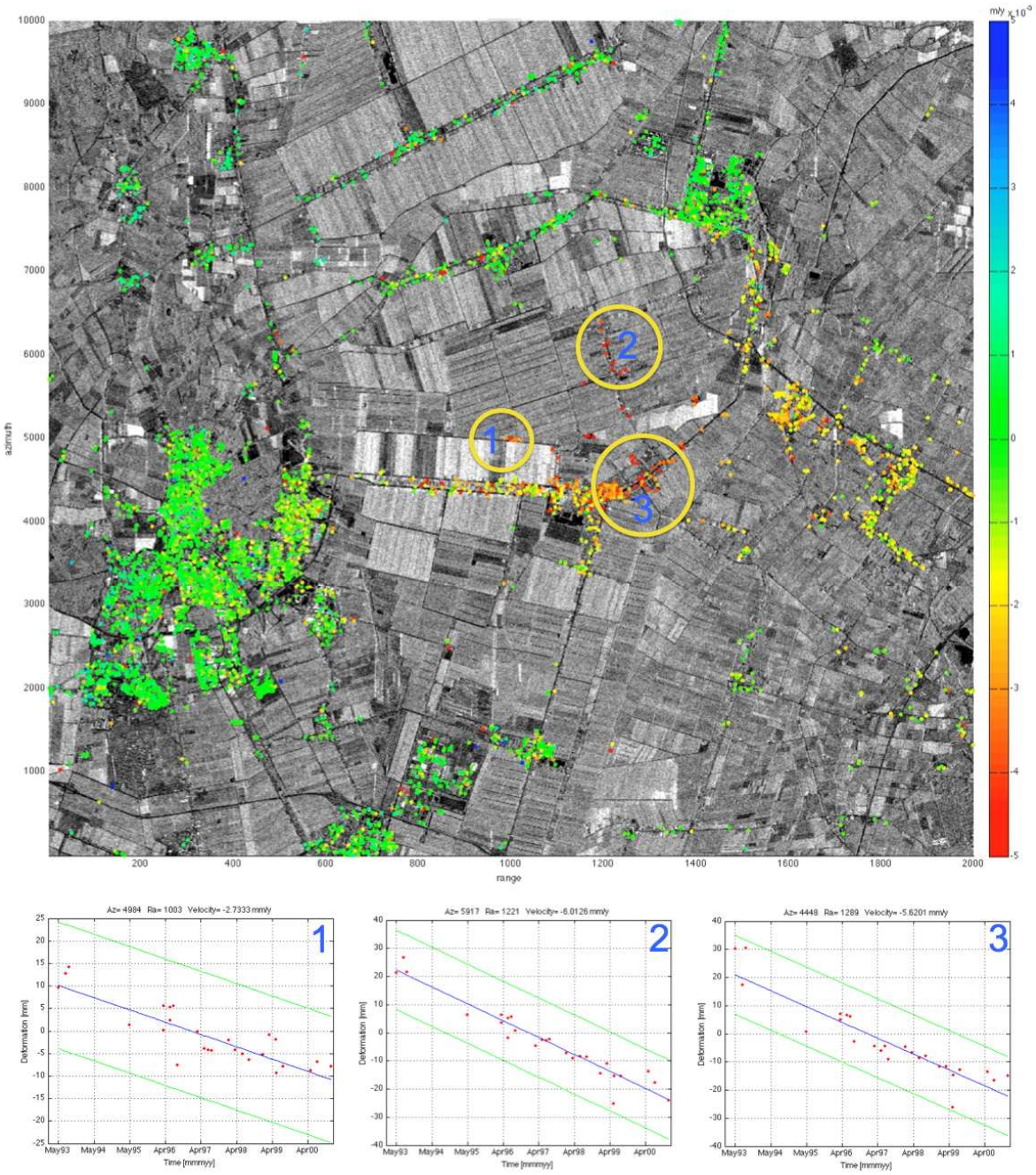

Figure 8. PS deformation map of the Roswinkel area using ascending track 380, showing the deformation time series of representative PS points in the subsidence bowl.

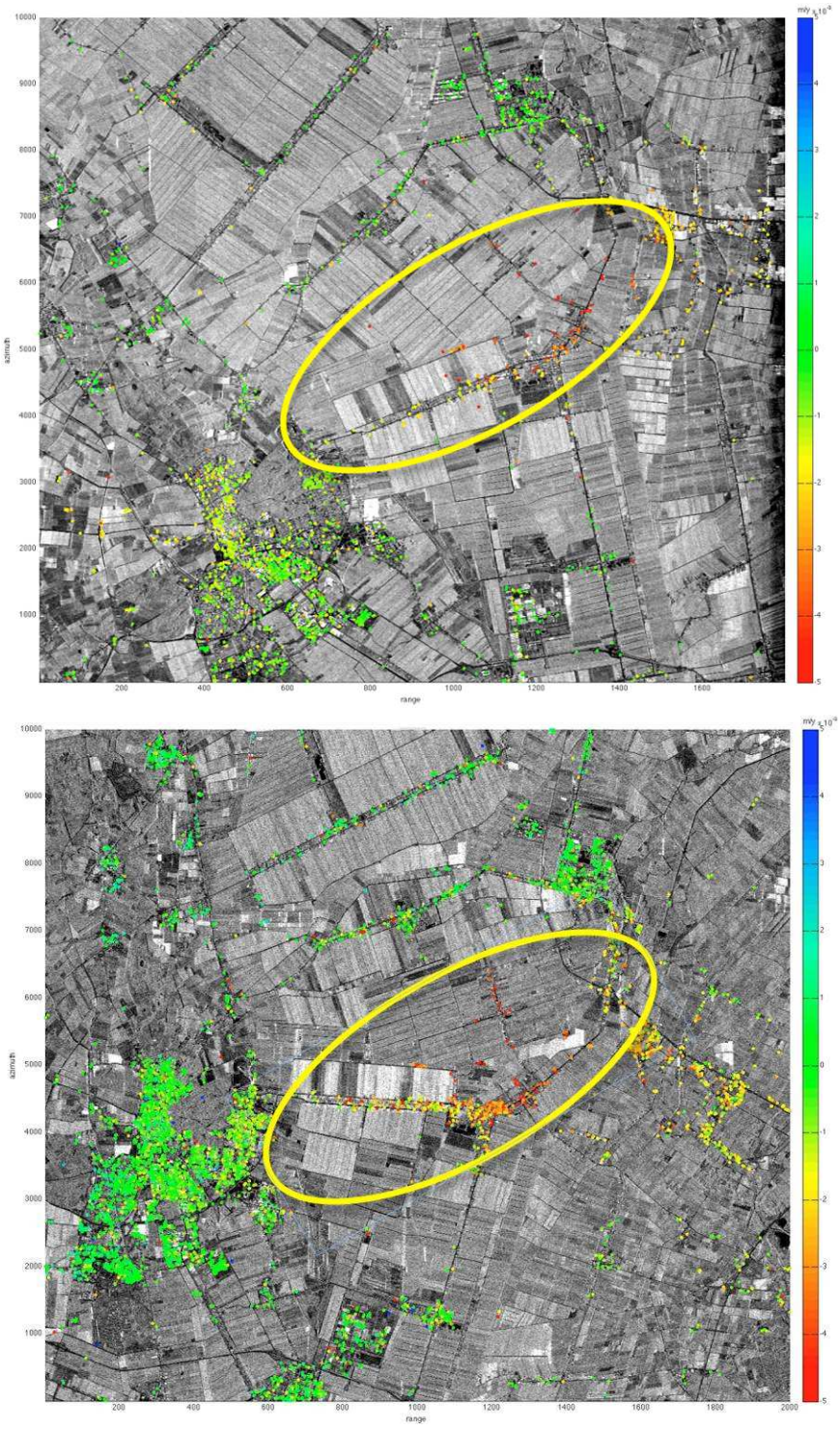

Figure 9. Comparison between the PS deformation maps of Roswinkel from descending track 215 (top) and ascending track 380 (bottom). The rough subsidence zone is highlighted. Note the sparse coverage of PS points on parts of the subsidence zone.

5 The Barendrecht case

5.1 Background

As part of CATO2, it is proposed that CO_2 be injected into two depleted gas fields in the Barendrecht area for permanent storage. At the smaller Barendrecht field, 800,000 tonnes of CO_2 are intended to be stored at a depth of 1.7 km, and the larger Ziedewij field can store 9.5 million tonnes of CO_2 at a depth of 2.7 km. 10 million tons of CO_2 are planned to be stored in this area over a period of 25 years. These wells are located at some distance from residential areas, and Figure 10 shows a view of the Barendrecht gas field and its surroundings [Luca 2010]. Gas production in the single well at Barendrecht will stop in 2010, and four wells in Ziedewij will stop producing gas in 2014. CO_2 sequestration is planned in these wells after their depletion. These wells were chosen owing to their well-known geological characteristics, minimized risk of leakage (few wells) and proximity to CO_2 source (limited transport costs and risks).

Figure 10. A view of the Barendrecht gas field area.

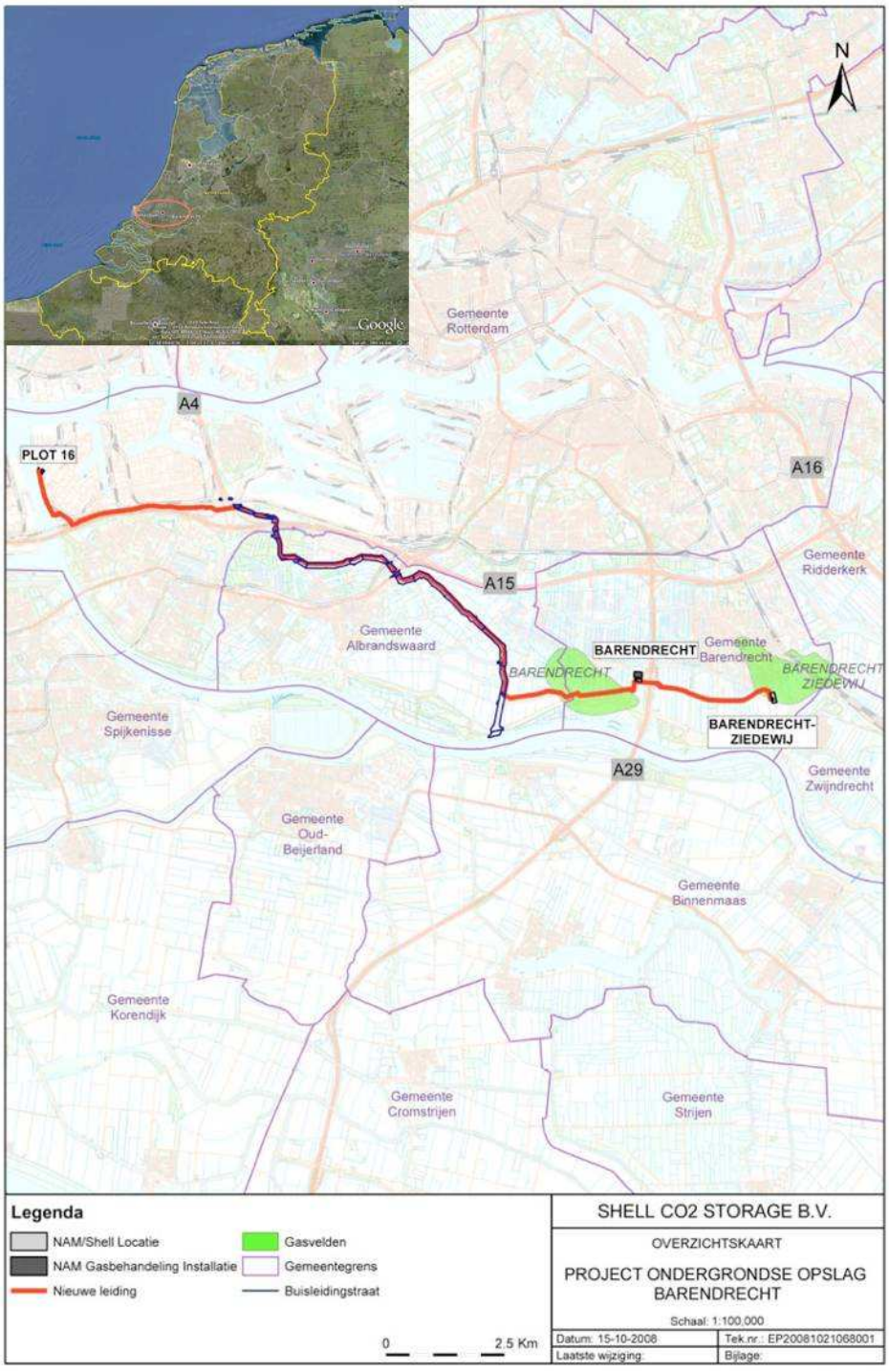

Figure 11. Location of the Barendrecht and Ziedewij gas fields (see inset for location within the Netherlands).

5.2 PSI processing of Barendrecht (ERS, 1992-2002)

ERS descending track data in the period 1992-2002 over Zuid Holland were used to study the deformation in the Barendrecht area. The crop is centred at 51.8546°N and 4.5523°E. 84 SAR image acquisitions were used for PSI processing, with the master acquisition on 14 May 1997. The reference point is at 52.4254°N and 5.3833°E.

Table 2. Acquisition dates (time series) of ERS descending tracks (master on 14 May 1997).

26-APR-1992	20-MAR-1996	06-OCT-1999
31-MAY-1992	24-APR-1996	10-NOV-1999
05-JUL-1992	28-MAY-1996	14-DEC-1999
09-AUG-1992	29-MAY-1996	15-DEC-1999
13-SEP-1992	03-JUL-1996	18-JAN-2000
18-OCT-1992	06-AUG-1996	19-JAN-2000
22-NOV-1992	07-AUG-1996	22-FEB-2000
27-DEC-1992	11-SEP-1996	23-FEB-2000
31-JAN-1993	20-NOV-1996	29-NOV-2000
07-MAR-1993	25-DEC-1996	01-AUG-2001
11-APR-1993	29-JAN-1997	19-DEC-2001
16-MAY-1993	09-APR-1997	03-APR-2002
20-JUN-1993	18-JUN-1997	
25-JUL-1993	23-JUL-1997	
29-AUG-1993	27-AUG-1997	
03-OCT-1993	01-OCT-1997	
07-NOV-1993	05-NOV-1997	
04-APR-1995	10-DEC-1997	
09-MAY-1995	14-JAN-1998	
13-JUN-1995	18-FEB-1998	
18-JUL-1995	25-MAR-1998	
19-JUL-1995	29-APR-1998	
22-AUG-1995	03-JUN-1998	
23-AUG-1995	08-JUL-1998	
26-SEP-1995	12-AUG-1998	
27-SEP-1995	16-SEP-1998	
31-OCT-1995	21-OCT-1998	
01-NOV-1995	25-NOV-1998	
05-DEC-1995	30-DEC-1998	
06-DEC-1995	03-FEB-1999	
09-JAN-1996	10-MAR-1999	
10-JAN-1996	14-APR-1999	
13-FEB-1996	19-MAY-1999	
14-FEB-1996	23-JUN-1999	
19-MAR-1996	28-JUL-1999	

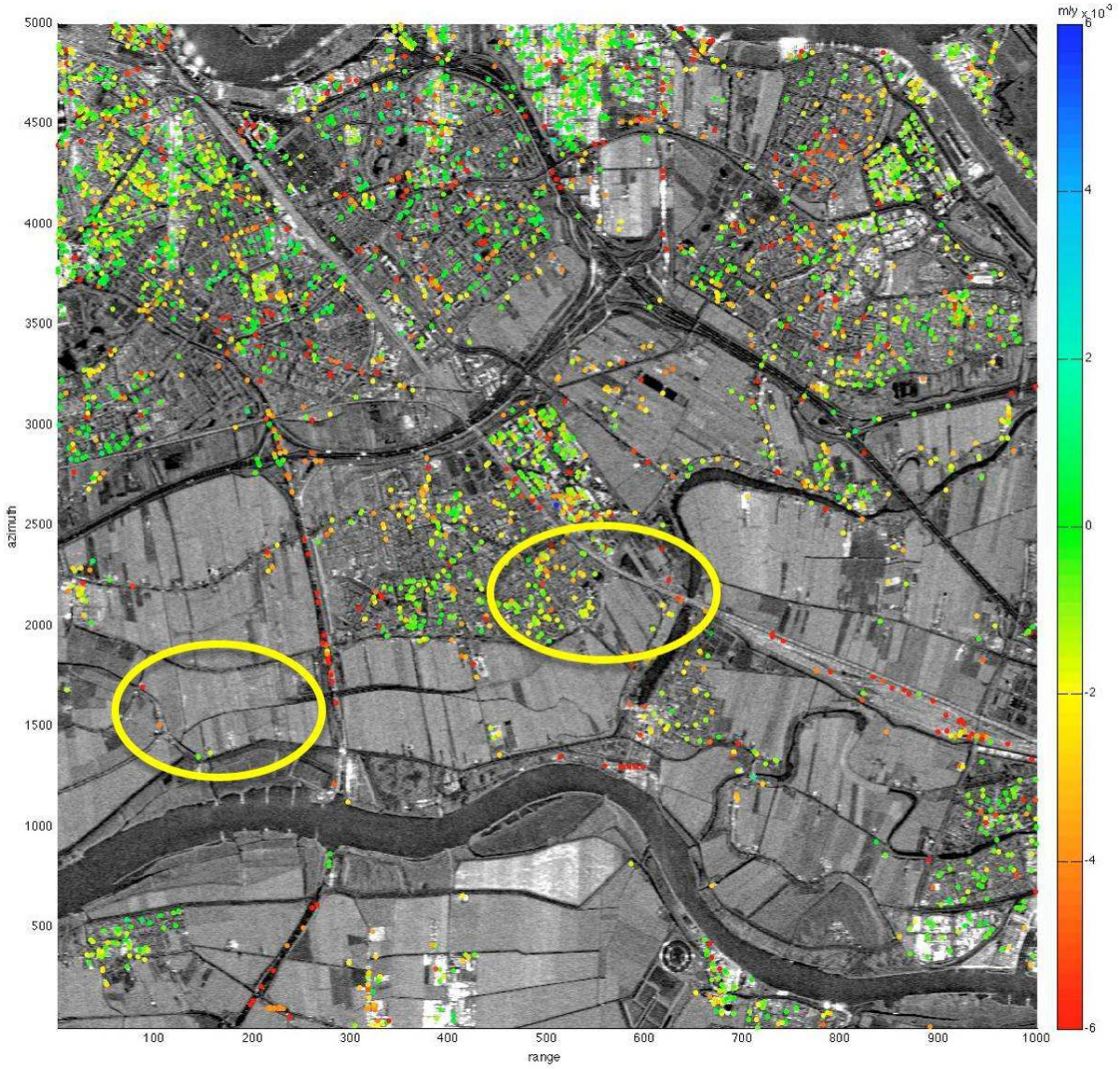

Figure 12. PS map using ERS data, highlighting the Barendrecht (left) and Ziedewij (right) gas fields. Note the absence of PS points on and around the Barendrecht field, and the sparse coverage of PS points on parts of the Ziedewij field for the time period 1992-2002.

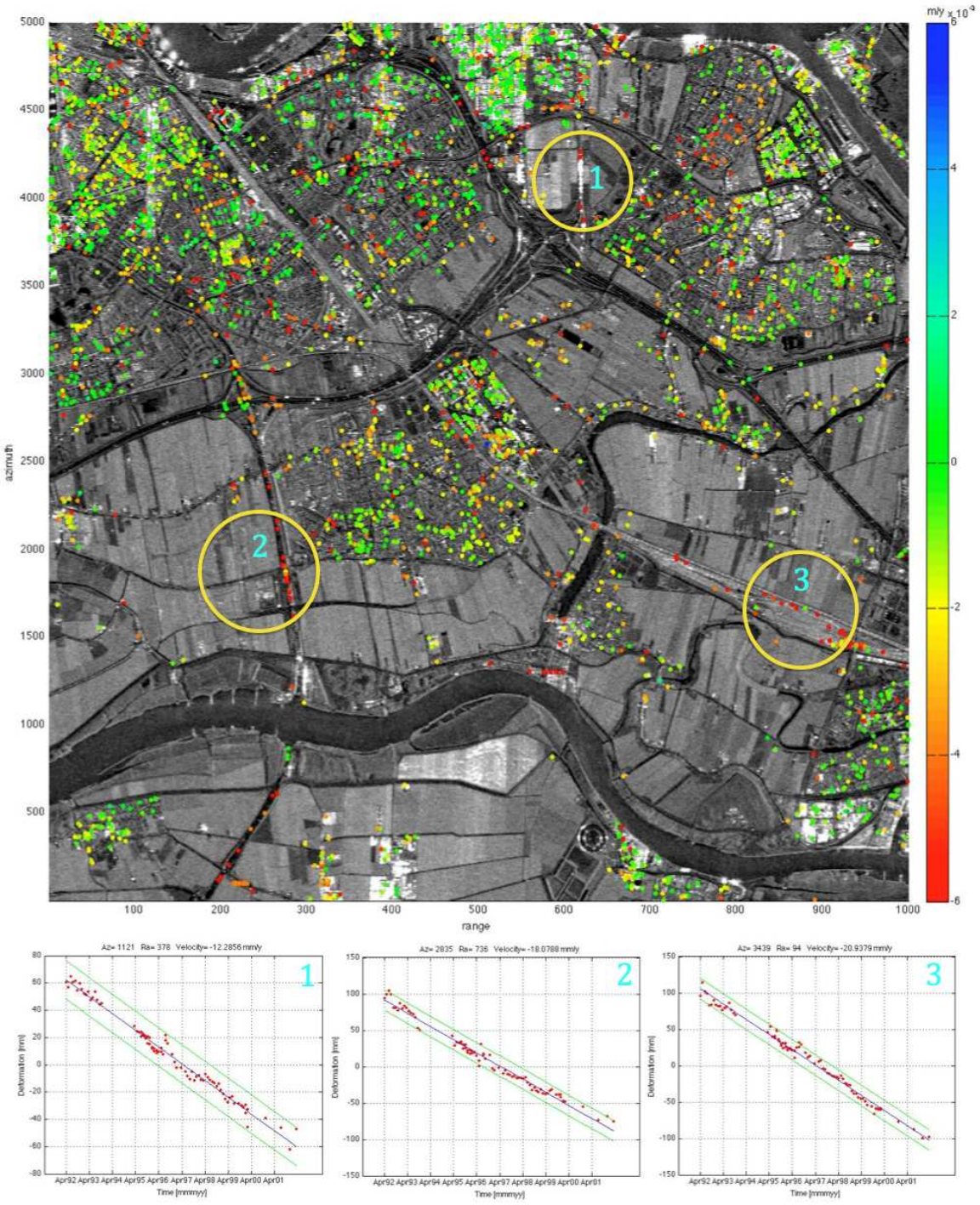

Figure 13. PS deformation map of the Barendrecht area using ERS data, showing the deformation time series of representative PS points in the area. Note that these signals are partly due to infrastructure-related ground compaction.

5.3 PSI processing of Barendrecht (Envisat, 2003-2010)

Envisat ASAR descending track data in the period 2003-2010 over Zuid Holland were used to study the deformation in the Barendrecht area. The crop is centred at 51.8546°N and 4.5523°E. 72 SAR image acquisitions were used for PSI processing, with the master acquisition on 21 Feb 2007. Table 3 lists the acquisition dates of Envisat ASAR. The reference point is at 52.4035°N and 5.6063°E.

Table 3. Acquisition dates (time series) for Envisat descending track (master on 21 Feb 2007).

12-FEB-2003	28-MAR-2007
02-JUL-2003	02-MAY-2007
06-AUG-2003	06-JUN-2007
10-SEP-2003	11-JUL-2007
15-OCT-2003	15-AUG-2007
19-NOV-2003	19-SEP-2007
24-DEC-2003	24-OCT-2007
28-JAN-2004	28-NOV-2007
03-MAR-2004	02-JAN-2008
07-APR-2004	06-FEB-2008
12-MAY-2004	12-MAR-2008
16-JUN-2004	16-APR-2008
21-JUL-2004	21-MAY-2008
25-AUG-2004	25-JUN-2008
29-SEP-2004	30-JUL-2008
03-NOV-2004	03-SEP-2008
08-DEC-2004	08-OCT-2008
12-JAN-2005	12-NOV-2008
16-FEB-2005	17-DEC-2008
23-MAR-2005	21-JAN-2009
27-APR-2005	25-FEB-2009
01-JUN-2005	01-APR-2009
06-JUL-2005	06-MAY-2009
10-AUG-2005	10-JUN-2009
19-OCT-2005	15-JUL-2009
23-NOV-2005	19-AUG-2009
28-DEC-2005	23-SEP-2009
01-FEB-2006	28-OCT-2009
08-MAR-2006	02-DEC-2009
21-JUN-2006	06-JAN-2010
26-JUL-2006	10-FEB-2010
30-AUG-2006	17-MAR-2010
04-OCT-2006	21-APR-2010
08-NOV-2006	26-MAY-2010
17-JAN-2007	

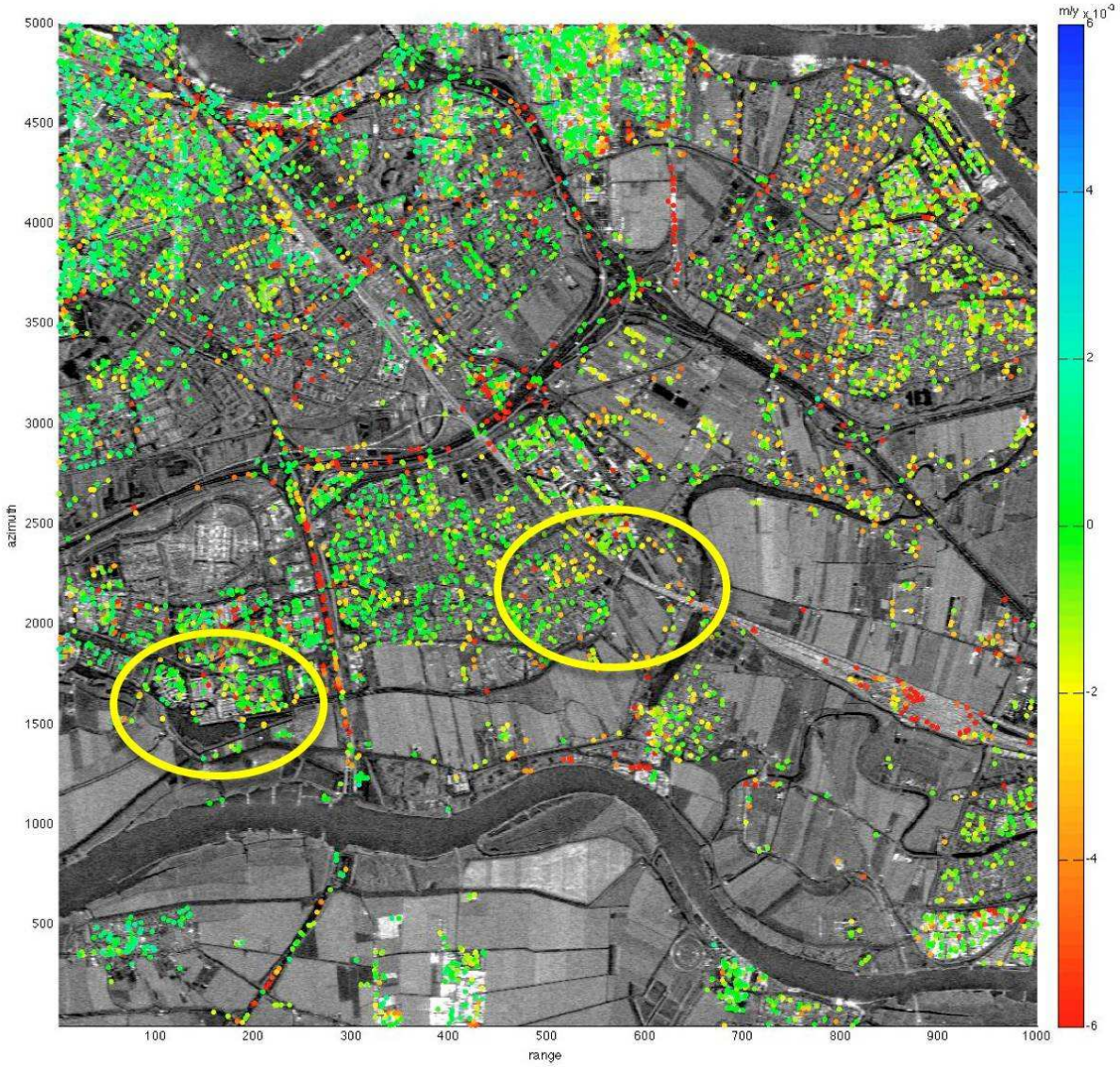

Figure 14. PS map using Envisat data, highlighting the Barendrecht (left) and Ziedewij (right) gas fields. Note the sparse coverage of PS points on parts of both fields, as well as in large areas in the southern and eastern parts of the image. The development of new residential areas before this period (2003-2010) yields many more PS points compared to ERS data of the previous decade (see Figure 12).

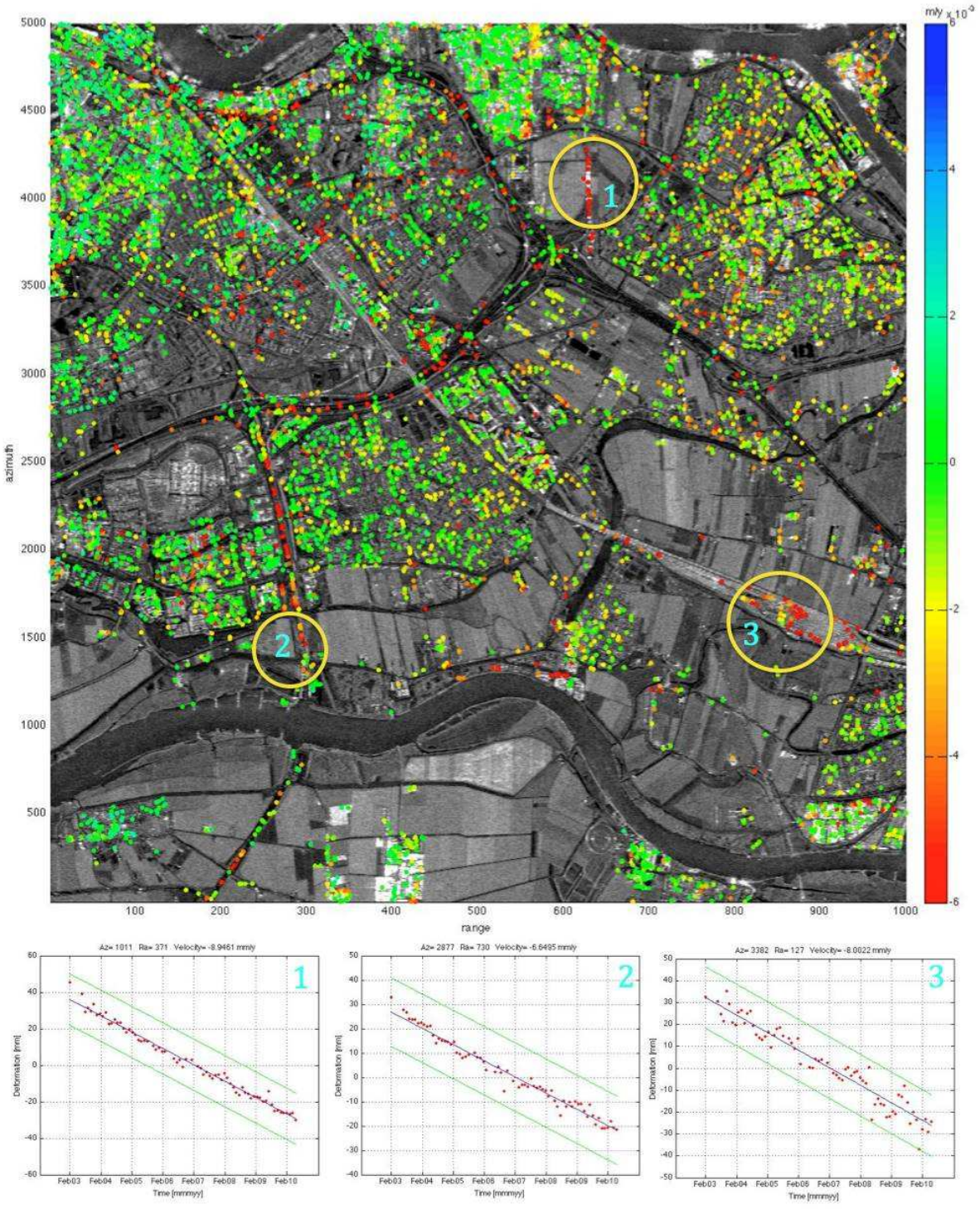

Figure 15. PS deformation map of the Barendrecht area using Envisat data, showing the deformation time series of representative PS points in the area.

The PS network forms a monitoring tool with a high spatial density of measurements, a kind of ‘‘natural geodetic network’’. However, the above PS maps show that large parts of the area of interest, i.e. on and around the gas fields, have sparse PS points. Interpolation techniques may be applied in order to estimate a deformation model for the region. However, the accuracy of such a model would depend heavily on the *a priori* assumptions made, and would be limited by the large areas with no PS point present.

6 An integrated monitoring approach

The two field cases performed allow a number of conclusions to be made:

- The Roswinkel case shows that it is possible to use PSI to observe surface movement
- The PS distribution can be suboptimal, especially in rural areas and in areas where infrastructural construction works are performed
- Surface movement monitoring needs to be combined with subsurface modelling to allow sensible conclusions about the static and dynamic behaviour of the subsurface (i.e. the movement of CO_2).
- When the surface movement is small, coming to determinate conclusions is problematic

As a result, it proofs to be necessary to come to an integrated approach in which different technologies are combined. Such integration can be achieved on different levels, which are exemplified in the present chapter.

6.1 Integration of PSI with GPS

A first possible way of improving the accuracy of deformation monitoring is by using GPS receivers as “artificial” geodetic benchmarks. The two satellite geodetic techniques, InSAR (and PSI) and GPS, work in remarkably similar ways, both utilizing the phases of electromagnetic waves to resolve the precise distance between the satellites and ground targets. The capabilities of the two techniques complement each other; while GPS can provide a 3D deformation vector at each GPS station with an accuracy of a few mm, InSAR can estimate the line-of-sight component of ground deformation over a large area at spatial resolution of tens of metres with mm accuracy. GPS coordinates can be considered as being 'absolute' in the sense that they are tied to a well-defined terrestrial reference system. On the other hand, InSAR results are 'relative' measurements. InSAR results, with their high spatial resolution, can be used to densify GPS results in a spatial sense [Ge et al]. The InSAR-GPS complementarity is summarized in Table 4.

Table 4. Complementarity of InSAR and GPS

InSAR	GPS
Low temporal resolution (several days)	High temporal resolution (30 s)
High spatial resolution (a few m)	Low spatial resolution (usually a few km between receivers)
Wide area coverage	Area coverage is localised
Line-of-sight deformation measurement	3D deformation measurement
Measurement accuracy of a few mm	Measurement accuracy of a few mm
No hardware or maintenance cost	High hardware and maintenance cost
Relative reference system	‘Absolute’ reference system

A novel system called I2GPS [Mahapatra 2010] is being developed which combines a Compact Active Transponder (CAT) and a GPS receiver to physically link the point-positioning capabilities of GPS with the very precise relative displacements as measured by InSAR. The instrument aims at integrating the antenna of a GPS receiver with a CAT antenna to ensure millimetric co-registration and assure a coherent cross-reference between the two precision surveying techniques.

Figure 16. An installed I2GPS unit in a landslide risk area for deformation monitoring (image courtesy of GeoZS).

Some prior approaches in literature to combine GPS and InSAR data are depicted schematically below, and follow two steps:

1. Sparse GPS measurements are interpolated to fill in GPS displacements in the InSAR grid.
2. 3D surface displacement maps are estimated using a suitable optimization technique.

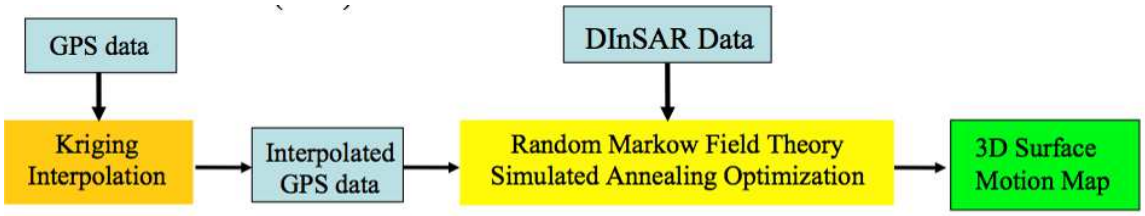

Figure 17. Algorithm by Gudmundssen et al. (2002) [Guglielmino et al.]

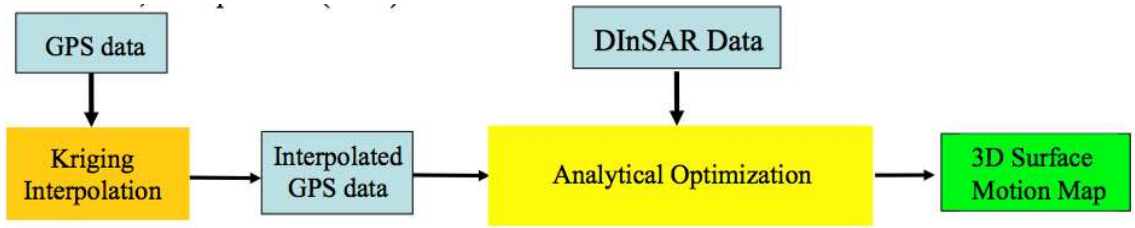

Figure 18. Algorithm by Samsonov, Tiampo et al. (2006) [Guglielmino et al.]

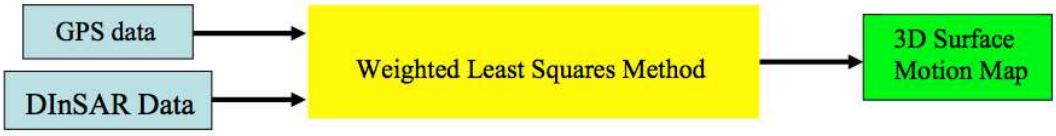

Figure 19. SISTEM by Guglielmino, Nunnari et al. (2009) [Guglielmino et al.]

In one such approach, since the deformation measured at a GPS station can be considered more reliable than InSAR (given its susceptibility to atmospheric delays, noise etc.), GPS data are inverted adopting classical formalisms [e.g. Mogi, Okada, Geertsma 1973]. The surface deformation pattern obtained from this first model is then used to compute a synthetic interferogram, which is compared to the experimental InSAR data. Finally, through trial-and-error, an acceptable model that jointly fits both GPS and InSAR datasets can be obtained [Palano 2008].

Another such approach proposes a distribution model for interpolation based on both GPS and InSAR results. In this Double Interpolation and Double Prediction (DIDP) approach, the GPS observations separated by one or several InSAR repeat cycles are densified in a grid manner by interpolation in the spatial domain based on the InSAR results; and then the densified grid observations are interpolated in the time domain using the 30 s sampling rate of the GPS time series. Adaptive filtering based on the least-mean-square algorithm is used to extract the dynamic model for this interpolation. While some sites of interest have both GPS and InSAR measurements of deformation, most other sites have only InSAR-derived results. It is important to have overlapping GPS and InSAR results so that the GPS results can be used to calibrate out some errors in the InSAR results. To derive the distribution model for interpolation in spatial domain, GPS sites are first matched with their imaging points in the InSAR result. The GPS displacements are subsequently projected to the change in range in the satellite line of sight.

Meanwhile, the InSAR result is resampled. Both the InSAR and GPS results are then least-squares adjusted as described above [Ge et al, 2000].

SISTEM (Simultaneous and Integrated Strain Tensor EstiMation) uses a least squares approach to derive 3D surface motion maps, which take both sparse Global Positioning System (GPS) measurements and Differential Interferometric Synthetic Aperture Radar (DInSAR) interferograms into account. SISTEM does not require preliminary interpolation of the observed deformation pattern, because it is based on a linear matrix equation that accounts for both GPS and DInSAR data. Thus, the estimation problem can be solved using the Weighted Least Squares (WLS) approach, thereby avoiding complicated search schemes such as simulated annealing optimization algorithm. Additionally, the solution of the linear matrix equation provides the strain tensor, displacement field and rigid body rotation tensor simultaneously within the entire investigated area [Spata 2009].

The absolute vertical velocity of the PSI image reference point in a well- defined reference frame [Zerbini 2007] can be achieved by collocating a GPS antenna with a radar corner reflector at the image reference point. On the other hand, the spatial information provided by PSI will be invaluable for determining the appropriate collocation point within the area of study. Another issue concerning the combination technique is the choice of the optimal spatial distribution of the GPS sites in a region, which would be required to support PSI analysis. Such a realization will be a key element for systematically understanding local ground deformation phenomena that may result due to CO_2 sequestration.

6.2 Inversion

The Roswinkel inversion study with levelling data shows that surface movement monitoring can be used as a means to collect knowledge about the static and dynamic subsurface characteristics. Due to the size of the signal and its lateral extent, all available knowledge needs to be taken into account. This prior knowledge concerns the expected level of pressure change in the reservoir, the mechanical response to these changes in the form of compaction, and the propagation of compaction to the surface, where it causes the surface movement. The surface movement has three independent components: one in the vertical direction and two in the horizontal directions. This immediately highlights the importance of having lateral displacement measurements as well. These can be obtained by combining InSAR measurements from different tracks, and of using GPS data.

For the subsurface input, a key element of the prior knowledge is the reliability of the expected compaction. This reliability is contained in the range of expected values, and, as importantly, in the correlations between the values at different locations. For that reason, the use of an ensemble of possible prior realizations was very useful. Such an ensemble naturally contains the required correlations.

The PSI study demonstrates that it is possible to observe high-quality surface movement data in persistent scatterers, of which the density and the location depends the local circumstances. The inversion technology applied to levelling data now has to be applied to PSI data. An assessment of solely using PSI data and of using PSI data in conjunction with levelling data will give insight in the added value of combining PSI with point source information collected by GPS.

In addition to inversion algorithms for surface movement data, algorithms exist, developed by TNO, for computer assisted history matching aimed at reservoir characterization. These algorithms can be used for well data (typically rates and well pressures). The information content of well data, however, is usually limited to the near-well region; injectivity can be inferred, but for

structural quantities global information is required. The Roswinkel inversion study can thus be further improved by the use of well data to constrain absolute pressures in the reservoir. We expect that large improvement in reservoir characterization can be achieved by integrating the use of improved geodetic information using PSI in the existing history matching techniques to allow the use of land surface movement data in combination with well data.

6.3 Integration of PSI processing and geophysical inversion

Space geodetic techniques like PSI greatly increase the possibility of improving geophysical knowledge of the subsurface, by applying inversion of subsidence data. However, the underlying geodetic data are actually results of an inversion as well, by processing satellite radar data. There are thus two independent estimation processes involved to relate the satellite data to the subsurface. Two problems beset these geodetic and geophysical inversions.

- In the geodetic inversion, an important limitation is the phase ambiguity estimation, It is nearly impossible to resolve the phase ambiguities correctly and unambiguously, especially when a strong and temporally complex deformation signal occurs in combination with an incomplete time series of radar acquisitions. Although the problem seems trivial, it is what mainly hampers practical applications of geodetic inversion and its acceptance by authorities.

- The second problem is that the end users (e.g. reservoir engineers) tend to use the estimated deformations from InSAR as deterministic input for modelling reservoir behaviour. For example, suppose that a single isolated scatterer is crucial for the reservoir modelling. As long as the reservoir engineer has no means to assess the quality of that particular measurement point, he will be inclined to discard it, as otherwise it would steer the solution of the inversion.

We contend that the two inversions, geodetic and geophysical, are not independent: knowledge of the physical reservoir behaviour might aid the phase ambiguity resolution, whereas a correct stochastic description of the InSAR data will improve the quality of the estimated reservoir parameters. The direct integration of space-geodetic and geophysical inversion techniques will significantly improve the ability to understand, monitor, predict and control geophysical processes such as reservoir pressure development and surface subsidence because of the superior spatial and temporal density of the space-geodetic measurements. We will develop an integrated approach for the estimation of geophysical parameters, combining physical modeling and space geodetic observations, particularly aimed at reservoir studies. The approach will be constructed from the integrated procedure for the inversion of subsidence measurements as demonstrated on the Roswinkel case, and the InSAR methodology presented above.

One problem is that the sampling of the time series is not always attuned to the deformation behaviour, e.g. due to missing acquisitions. Also, the data are subject to different types of correlation. Spatial correlations occur as a result of oversampling, sidelobes and atmosphere. Temporal sources of correlations are DEM errors, elevation-dependent atmosphere and the foundations under the reflecting infrastructure. Integer phase ambiguities need to be resolved both spatially and temporally. A sparse grid of coherent scatterers measured infrequently makes it difficult to resolve ambiguities reliably. Our integrated inversion procedure would address these problems by adding the a priori physical information to the geodetic estimation problem. Thus, key to this procedure is the integration of information from PS-InSAR and the geological processes. If necessary, we will combine the PS-InSAR data with other types of data, to improve the quality of the procedure even more. Finally, the non-linearity of the forward model hampers a simple inversion. The non-linear inversion or data assimilation methodology that we envisage will

treat the non-linearity, the integer phase ambiguity, the correlations and the uncertainties in an integrated way. The proposed approach is an intimate mathematical integration, removing the thresholds induced by the staged application of estimation techniques; it is also a truly multidisciplinary development, in which geophysical estimation and inversion becomes much more efficient thanks to a deeper mutual understanding of the requirements and possibilities of the contributing disciplines. We anticipate that this integrated approach will significantly change our ability to quantify the underlying processes and parameters, even making it possible to use space-geodetic data in inversion studies where this is currently impossible.

We will cast the two estimation problems in a single mathematical model, enabling proper procedures for error propagation. The inversion of these joint mathematical models can then be tested using different methods, such as best linear unbiased estimation, Bayesian approaches, or least-squares collocation. We will tackle the phase ambiguity resolution for all the data via the likelihood of the estimated ambiguities: alternative, highly likely, ambiguities will be retained, thus ensuring that the information contained by the lower-order likelihoods is kept in the estimation routine. Following this, there is the option of directly estimating ambiguity using the integer least-squares approach ('lambda method') or of evaluating the sensitivity of the inversion to alternative estimated ambiguities. This involves moving away from classical inversion to an assumption of a more intimate relationship between measured data and model parameters.

More specifically, the data assimilation exercise aims at solving $\mathbf{d} \approx \mathbf{G.m}$ for $\mathbf{m}$, under the constraint that $\mathbf{m} \approx \mathbf{m}_0$, in which $\mathbf{d}$ are the data, $\mathbf{G}$ the forward physical model, $\mathbf{m}$ the unknown parameters, and $\mathbf{m}_0$ the prior knowledge about these parameters [Menke 1989]. We will use the direct line-of-sight phase observations from InSAR as input. Crucial input in the inversion are the covariance matrices of both the prior model $\mathbf{m}_0$ and of the data, $\mathbf{d}$. As InSAR produces large amounts of data, these matrices will not necessarily be inverted directly, but as a functional of the much simpler underlying covariance functions.

The covariance matrix of the data needs to be derived from the information on the data collection procedure. In this context, it is important to note that the selection of persistent scatterers (PS points) for InSAR is a computationally expensive exercise. We intend to also use the integrated inversion methodology to provide a feedback loop to the result of this selection. The results of an inversion can be used to estimate the quality of the PS points. From this we can optimize the selection of the PS points and obtain a better idea about their dispersion. Iterative loops may be an essential ingredient in the estimation procedure.

The covariance matrix of the prior parameter model is also prior information. It contains the uncertainty of the prior estimates of the parameters, and, just as importantly, the correlations between them. We will derive the covariance by running Monte Carlo simulations and varying the driving parameters.

The data assimilation technology will be tested first on synthetic data. This ensures maximum controllability of the process, as the outcome of the exercise can be compared with the synthetic truth. Earlier studies have shown that such an approach can yield important insights specific for the inversion problem at hand and the specific features of the field [Muntendam et al., 2008; Kroon et al., 2009]. After the inversion of the synthetic data has been completed, the methodology will be applied to real data. We expect this to yield major new insights into aquifer activity and the interference between deep and shallow compaction processes.

7 Bibliography

Burgmann, R., Hilley, G., Ferretti, A. and Novali, F. “Resolving vertical tectonics in the San Francisco Bay Area from permanent scatterer InSAR and GPS analysis.” *Geology*, 2006.

Fokker, P., Visser, K., Peters, E., Kunakbayeva, G. and Muntendam-Bos, A. “Inversion of surface subsidence data to quantify reservoir compartmentalization: A field study.” SPE paper 134457, to be presented at the Ann. Tech. Conf & Exh of the SPE< Florence, September 2010.

Ge, L., Han, S. and Rizos, C. “Interpolation of GPS results incorporating geophysical and InSAR information .” 1999.

Ge, L., Han, S. and Rizos, C. “The Double Interpolation and Double Prediction (DIDP) approach for InSAR and GPS integration.” *International Archives of Photogrammetry & Remote Sensing* , 2000.

Ge, L., Rizos, C., Han, S. and Zebker, H. “Mining subsidence monitoring using the combined InSAR and GPS approach.”

Geertsma, J. “A basic theory of subsidence due to reservoir compaction: the homogeneous case”, *Verh. Kon. Ned. Geol. Mijnbouwk. Gen. 28, p. 43-62*

Guglielmino, F., Nunnari, G. , Puglisi, G. and Spata, A., “Simultaneous and Integrated Strain Tensor Estimation from geodetic and satellite deformation Measurements”, *FRINGE 2009*, http://earth.eo.esa.int/workshops/fringe09/participants/870/pres_870_Spata.pdf

Kampes, B. and Usai, S. “Doris: the Delft Object-oriented Radar Interferometric Software.” *2nd International Symposium on Operationalization of Remote Sensing*, 1999.

Ketelaar, V. “Monitoring surface deformation induced by hydrocarbon production using satellite radar interferometry.” PhD Thesis, Delft University of Technology, 2008.

I.C. Kroon, B.-L. Nguyen, P.A. Fokker, A.G. Muntendam-Bos and G. de Lange: ‘Disentangling shallow and deep processes causing surface movement’ Math. Geosci., **41**, 571-584.

Luca, C. “Barendrecht CO2 Storage Project.” 2010. http://netherlands.spe.org/images/netherlands/articles/70/CCS%20Barendrecht%20SPE_PGK%2021%20June%202010%20webversion.pdf.

Mahapatra, P. *I2GPS: Integrated Interferometry and GNSS for Precision Survey.* 2010. http://www.i2gps.eu/.

Menke, W. “Geophysical data analysis: Discrete inverse theory”, Ac. Press, San Diego, 1989

Muntendam-Bos, A.G., I.C. Kroon, and P.A. Fokker: ‘Time-dependent inversion of surface subsidence due to dynamic reservoir compaction’ Math Geosci **40**, pp. 159–177

Palano, M., Puglisi, G. and Gresta, S. “Ground deformation patterns at Mt. Etna from 1993 to 2000 from joint use of InSAR and GPS techniques.” *Journal of Volcanology and Geothermal Research*, 2008.

Samiei-Esfahany, S. “Improving PS-InSAR results for deformation monitoring.” Master Thesis, Delft University of Technology, 2008.

Samiei-Esfahany, S., Hanssen, R., van Thienen-Visser, K. and Muntendam-Bos, A. “On the effect of horizontal deformation on InSAR subsidence estimates.” *FRINGE*, 2009.

Spata, A., Guglielmino, F., Nunnari, G. and Puglisi, G. “SISTEM: a new approach to obtain three-dimensional displacement maps by integrating GPS and DInSAR data.” *FRINGE*, 2009.

Zerbini, S., Richter, B., Rocca, F., van Dam, T. and Matonti, F. “A Combination of Space and Terrestrial Geodetic Techniques to Monitor Land Subsidence: Case Study, the Southeastern Po Plain, Italy.” *Journal of Geophysical Research*, 2007.